Morphology, crystallization and melting behaviour of films of isotactic polypropylene blended with ethylene–propylene copolymers and polyisobutylene

Ezio Martuscelli, Clara Silvestre and Giancarlo Abate
Istituto di Ricerche su Tecnologia dei Polimeri e Reologia del CNR, Via Toiano, 2, Arco Felice, Napoli, Italy
(*Received* 10 *November* 1980; *revised* 9 *March* 1980)

The crystallization, the morphology and the thermal behaviour of thin films of isotactic polypropylene (iPP) blended with elastomers such as random ethylene–propylene copolymers (EPM) with different ethylene content and polyisobutylene (PiB) were investigated by means of optical microscopy, differential scanning calorimetry and wide angle X-ray diffractometry. During crystallization EPM copolymers are ejected on the surface of the film forming droplet-like domains A different morphology is observed in iPP/PiB blends For these mixtures the elastomers separate from the iPP phase forming spherical domains that are incorporated in the iPP intraspherulitic regions. Both EPM and PiB elastomers act as nucleant agents for iPP spherulites. This nucleation efficiency is strongly dependent on the chemical structure and molecular mass of the elastomers. The addition of EPM causes an elevation of the observed and equilibrium melting temperature of iPP. This unusual effect may be accounted for by assuming that the elastomers are able to extract selectively the more defective molecules of iPP. The depression of the growth rate of spherulites and the observed and equilibrium melting temperature of iPP, noted in iPP/PiB blends, suggests that these two polymers have a certain degree of compatibility in the melt

Keywords Characterization; crystallization; morphology, thermal behaviour; polypropylene; copolymers;

INTRODUCTION

The use of various elastomers such as ethylene–propylene copolymers (EPM), ethylene–propylene–diene terpolymers (EPDM), butyl rubber (BR), polyisobutylene (PiB), styrene–butadiene (or isoprene)–styrene block copolymers (SBS or SIS elastomers) to improve the impact strength and the environmental stress-cracking resistance at normal and low temperatures of polyethylene (PE) and isotactic polypropylene (iPP), has been known, in commercial practice for many years.

Intensive research in this field led to the formulation of a new class of polymeric materials such as polyolefins modified with elastomers[1].

EPM rubbers have a lower glass transition temperature than iPP, the resulting blends show reduced rigidity improved toughness and impact strength. According to Horie *et al.*[2] EPM acts as plasticizer for iPP and PE blends.

In their studies Ermilowa *et al.*[3] found that EPM rubbers affect the flow properties and the low temperature properties of iPP and PE.

Impact modification of iPP with EPM and EDPM based elastomers have been the subjects of several patents. It has been shown by Kumbhoni[4] that butyl rubber is beneficial in improving environmental stress-cracking and impact resistance at low temperatures in PE and iPP. Spenadel[5] made an extensive study on the influence of rubber on the environmental stress-cracking resistance (*ESCR*) of PE. He found that on increasing rubber concentration the ESCR improved at the expense of decreased stiffness and melt flow. The extent to which *ESCR* can be improved was found to be highly dependent on the chemical nature of the added rubber and in the case of PiB also on molecular weight. The *ESCR* increases with increasing molecular mass of PiB.

Due to the crystallization process at temperatures below T_c, iPP(PE)/elastomer blends are generally heterogeneous. Thus their properties will depend on the overall morphology of the blend, i.e. the shape and size distribution of polyolefin spherulites and of rubbery domains, adhesion at the interface, nature and structure of the rubbery domains.

The overall morphology of the iPP/elastomers blends has been studied by Karger Kocsis *et al.*[6] by using wide and small angle X-ray diffractometry, small angle light scattering, light and electron microscopy and differential scanning calorimetry. The blends were prepared by extrusion and the test specimens were then injection moulded. From this investigation it emerges that:

(i) The incorporation of an elastomer alters the superstructure of iPP matrix by decreasing the average size of spherulites.

(ii) The mechanical properties are dependent on the interphase structure and on the size of the amorphous elastomer domains and iPP spherulites.

(iii) The impact modifiers act as nucleating agents for the iPP monoclinic phase and they seem to decrease the degree of iPP undercooling.

According to Karger–Kocsis *et al.*[6] above T_g the elastomer, by absorbing energy, influences the crazing susceptibility of the iPP matrix.

The blends of iPP and ethylene–propylene rubbers have been studied by Danesi and Porter[7] in order to

0032-3861/82/020229 09$03 00

Table 1 Molecular characteristics, source and code of the polymers used in the present investigation

Polymer	Source and trade names	Molecular mass	Viscosità Mooney ML (1 + 4) at 100°C	Ethylene propylene ratio (W/W)
Isotactic polypropylene (iPP)	RAPRA	$\bar{M}_W = 3.07 \times 10^5$ $\bar{M}_n = 1.56 \times 10^4$	–	–
Ethylene-propylene copolymers (EPM)	Dutral Co054 (Montedison)	–	43	60/40
	Buna AP201 (Huels)	–	44	50/50
	Epcar 306 (Goodrich)	–	34.5	>67/30
Polyisobutylene (PiB)	Vistanex L120 (Esso)	$\bar{M}_V = 1.6 \times 10^6$*	–	–

* Measured in cyclohexane at 30°C

establish relationships between morphology and physical properties and to examine the principles which govern the developments of morphologies. The influence of blending conditions on the dispersion state was also explored. The blends were prepared by using a Brabender single screw extruder in combination with a 'Static Mixer'. They were rheologically characterized using in Instron capillary rheometer. The mechanical and morphological characterization was performed directly on the extrudates obtained from the capillary rheometer.

Here the isothermal crystallization, the morphology and the thermal behaviour of thin films of iPP/elastomers blends were investigated to study the influence of the elastomer chemical structure and composition on the shape and size of the spherulites and rubbery domains, on the spherulite growth rates, on the equilibrium melting temperatures and the crystallinity of iPP phase.

EXPERIMENTAL

Materials

The characteristics of the polymers used in the present study are reported in *Table 1*.

Before blending, all polymers were purified as follows: they were dissolved in xylene at 120°C and washed with HCl (water solution 10% volume). Then they precipitated with methanol under a strong agitation, washed again with acetone and dried under vacuum at 80 C for 12 h to remove any water and residual solvent.

Preparation of blends

The binary blends of iPP with Dutral, Buna, Epcar and PiB at different compositions were prepared by using the following standard procedure: the two components were first dissolved in xylene at 120°C in the desired proportions; then the solvent was rapidly evaporated by using a rotavapor and the resulting powder dried under vacuum to remove any trace of solvent. Thin films (about 10 μ in thickness) were obtained by compression moulding of the blend powder at 200°C.

Radial growth rate measurements

The radial growth rates $G = dR/dt$ (R = radius of spherulites, t = time), were calculated by measuring the size of iPP spherulites as function of time during the isothermal crystallization process. An optical polarizing microscope fitted with an automatized hot stage was used. The hot stage could be held at a steady temperature to ±0.02°C by a proportional controller. The following procedure was used: blend films were sandwiched between a microscope slide and a cover glass, heated 20°C above the melting point of iPP and kept at this temperature for 10 min to destroy any trace of crystallinity; the temperature was then rapidly lowered to T_c and the blend allowed to crystallize isothermally.

Table 2 Blend compositions and range of crystallization temperature explored

Blend	Composition	Range of T_c explored
iPP/Epcar	95/ 5	119–139
	90/10	119–139
	80/20	119–137
iPP/Dutral	95/ 5	119–141
	90/10	119–141
	80/20	119–141
	70/30	119–141
iPP/Buna	90/10	119–139
	80/20	119–141
	70/30	119–135
iPP/PiB	90/10	119–135
	80/20	119–135

The photomicrographs were taken on the growing spherulites at appropriate intervals. The radius R was measured on print and G calculated as the slope of the straight lines obtained by plotting R against time.

The observed melting temperatures T'_m of iPP, crystallized from melt blends, were also measured by using the optical microscope by heating the film from T_c to T'_m at a rate of 10°C/min. The temperature at which birefringence disappeared was taken as T'_m.

Crystallinity measurements

The values of crystallinity X_c were determined calorimetrically by using a Perkin–Elmer (model DSC2-B) differential scanning calorimeter.

The crystallinity of the iPP phase in the blends was calculated by means of the following relation:

$$X_c^{iPP} = \frac{\Delta H^*_{iPP}}{\Delta H_{iPP}}$$

where ΔH^*_{iPP} is the apparent enthalpy of fusion per gram of iPP in the blend and ΔH_{iPP} is the heat of fusion of 100% crystalline iPP (from literature data $\Delta H^\circ_{iPP} = 50$ cal/g[8]). Observed melting temperatures T'_m were also determined from d.s.c. thermograms obtained by heating the samples from T_c to T'_m.

The compositions of the blend examined and the crystallization temperatures explored are reported in *Table 2*.

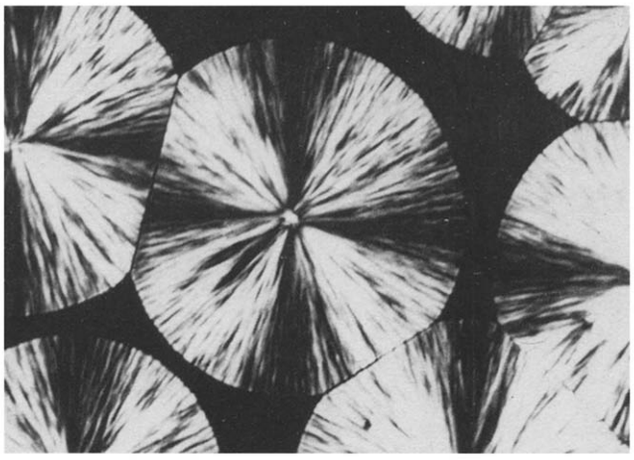

Figure 1 Optical micrograph of melt crystallized film of IPP (T_C = 125°C: crossed polars)

Wide-angle X-ray diffractometry

The wide-angle X-ray scattering was performed by means of a Philips PW 1130 diffractometer with proportional counter using Ni filtered CuKα radiation, in order to establish the presence, in the samples, of crystalline iPP in the hexagonal polymorphic form.

RESULTS AND DISCUSSION

Morphology

The overall morphology of iPP/EPM and iPP/PiB blends and the influence of composition, crystallization temperature and chemical structure of elastomer on the structure, size and shape of iPP spherulite were studied in detail by optical microscopy.

Birefringent spherulitic structures, truncated by impingement are observed when a thin film of iPP crystallizes from the melt isothermally. The birefringent patterns displayed a maltese cross whose arms are parallel to the directions of the analyser and polarizer (see *Figure 1*).

Optical micrographs of films of iPP/EPM and iPP/PiB blends are shown in *Figures 2* and *3*.

In the case of iPP/EPM blends the elastomers are ejected during crystallization, onto the surface of the film. Some large interspherulitic amorphous regions are also observed. As shown in *Figure 2* the domains of the elastomers, whose shape is mainly droplet like, are oriented along flow lines induced by the crystallization process. This is the reason why, giving rise to birefringence, they may be observed, on the surface of the films, under crossed polars. By annealing the films at temperatures higher than T_c, the strains are relaxed and the amorphous domains lose their birefringence properties. At these temperatures only the spherulitic structure of iPP phase is observed when the films are examined under the optical microscope with crossed polars (see *Figure 2c*).

As shown in *Figure 3*, a different overall morphology is observed for iPP/PiB blends. For this mixture the elastomer separates from the iPP phase forming spherical domains (with a diameter ranging from 3 to 5 μm) that are incorporated in the iPP intraspherulitic regions.

According to Stein *et al.*[9] the types of overall morphology observed in iPP/EPM and iPP/PiB blends

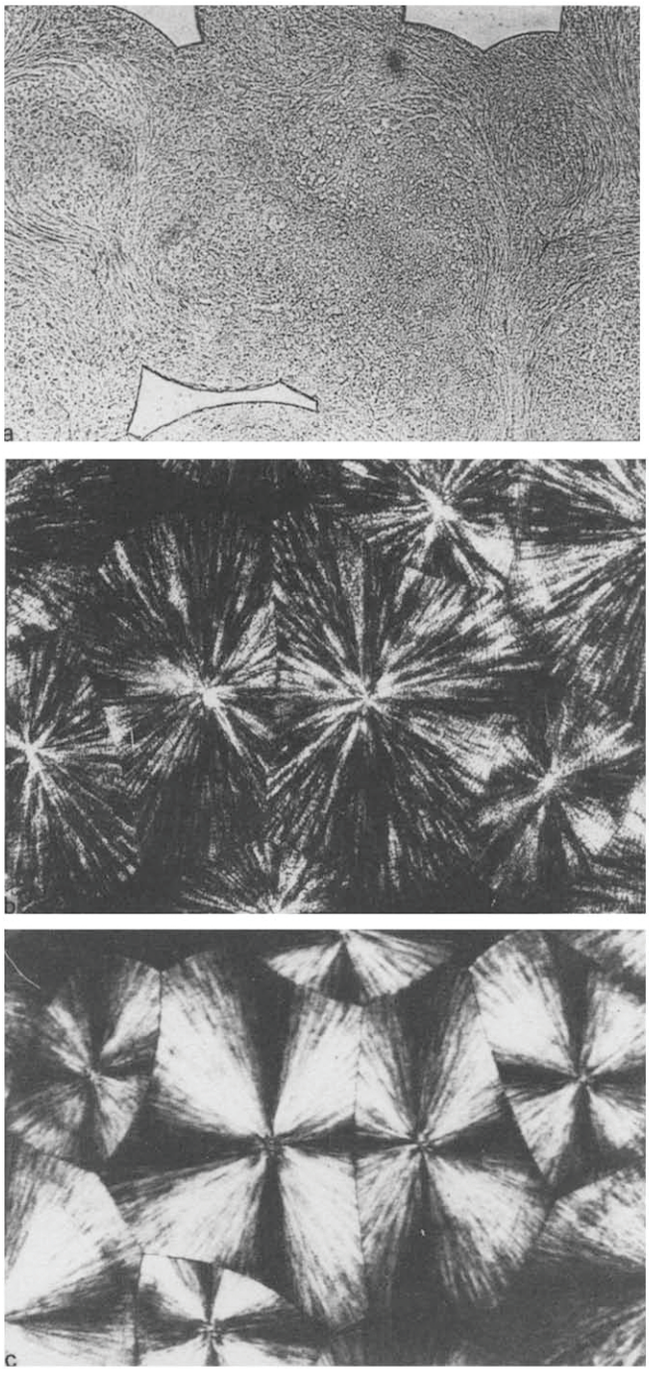

Figure 2 Optical micrographs of melt crystallized films of iPP/Buna (80/20) blends (a) T_C = 129°C, parallel polars; (b) T_C = 129°C, crossed polars; (c) T_C = 129°C, crossed polars after annealing at 157°C

could be related to the different values of the diffusion rates of EPM and PiB elastomers at the investigated crystallization temperatures.

As shown in *Figure 4*, the number of iPP spherulites per unit area (N/S), determined by light microscopy, increases with the addition of the elastomers. This effect is more marked in the case of iPP/Epcar blends.

In *Table 3* the values of N/S for blends containing 20% (by weight) elastomers are compared at three different crystallization temperatures (119, 125 and 131°C). The figures show that in the case of iPP/EPM blends for the same T_c and blend composition, N/S seems to increase with increasing ethylene content in the elastomer and with

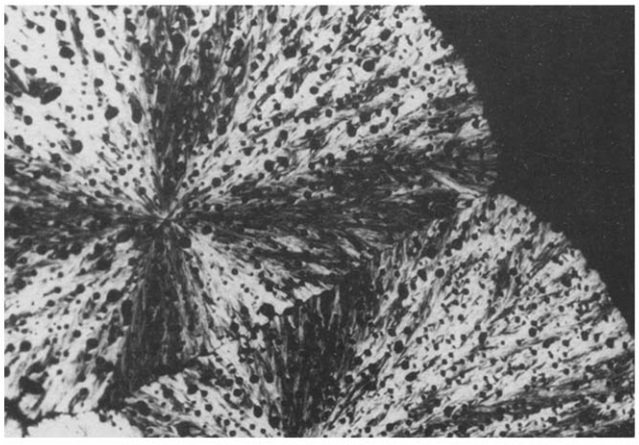

Figure 3 Optical micrograph of melt crystallized film of iPP/PiB (80/20) blend (T_c = 141°C, crossed polars)

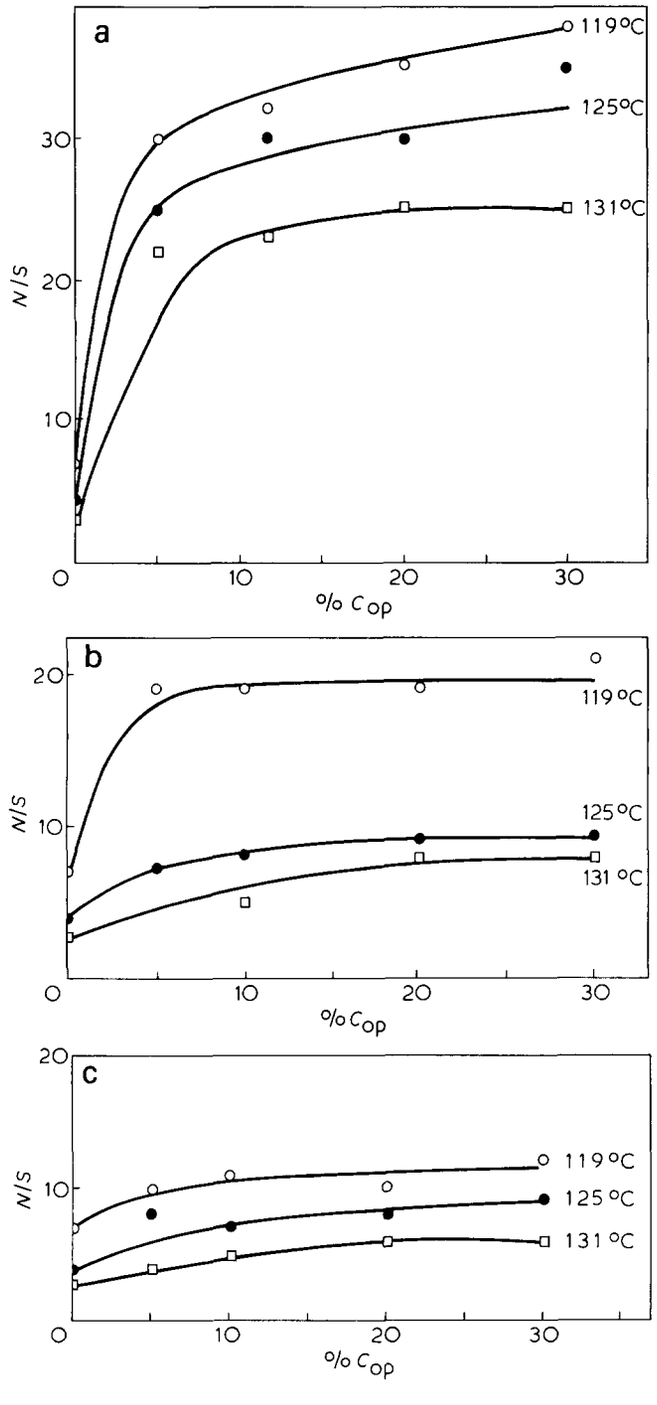

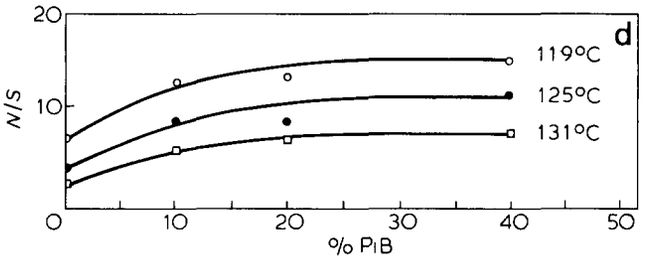

Figure 4 Number of spherulites per unit area *N/S* as function of elastomer content at three different T_c [119°, 125° and 131°C]: (a), iPP/Epcar blends; (b), iPP/Dutral blends; (c), iPP/Buna blends; (d), iPP/PiB blends

Table 3 Number of spherulites per unit area (*N/S*) at three different T_c for iPP/EPM and iPP/PiB (80/20) blends

Sample	T_c (°C) 119	*N/S* 125	131	Ethylene content in E/P copolymers (% W/W)
iPP/Epcar 80/20	34	28	23	>67
iPP/Dutral 80/20	19	9	7	60
iPP/Buna 80/20	9	7	5	50
iPP/PiB 80/20	12	7	5	–
iPP	7	4	3	–

decreasing molecular mass (see viscosity values in *Table 1*). For iPP/Epcar blends at 1250°C N/S is about 7 times that of iPP.

According to the above results we can conclude that EPM and PiB elastomers work as effective nucleating agents for iPP spherulites. Furthermore the nucleation efficiency of elastomers seems to be strongly dependent on their chemical structure and molecular mass.

A decrease in the size of iPP spherulites by addition of elastomers was observed also by Karger-Kocsis *et al.*[6] in injection moulded samples.

According to their results the average spherulite size of a sample containing 40% of EPM elastomer (Dutral Co054 by Montedison) is about 1/3 of the original iPP with a 67% reduction. Similar effects were found in blends containing styrene–butadiene–styrene block copolymer (SBS) (commercial grade, TR 1102 by Shell) and polyisoprene (commercial grade, Cariplex IR 305 by Shell) as elastomers. In these blends the addition of a 10% of elastomer causes a reduction in the size of spherulites of the 63% and 21% respectively.

Now it may be considered as established that the overall morphology and then the properties of blends of iPP and non crystallizing elastomers will depend to a considerable extent, not only on the composition, but also on the chemical structure of the amorphous component as well as on the molecular weight[10].

Radial growth rate of spherulites

The radius of iPP spherulites, crystallized from iPP/Dutral and iPP/PiB melt blends, as function of time is shown in *Figure 5* at a given T_c. The trend is linear in the whole range of investigated times. The values of the radial growth rates of spherulites G, in thin films of iPP, iPP/EPM and iPP/PiB blends are given in *Table 4* as

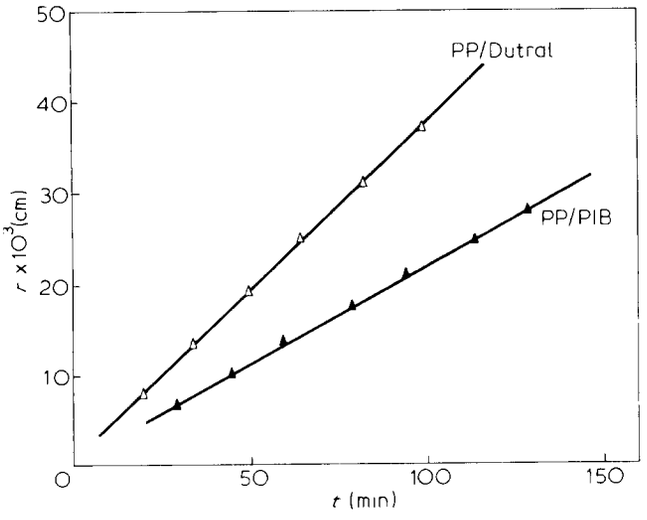

Figure 5 Typical plots of radius of iPP spherulites crystallized from melt blends as function of time (T_c = 131°C)

Table 4 Radial growth rate of iPP spherulites, $G \times 10^3$ (cm/min), as function of crystallization temperature and composition

	Percent of amorphous material in the blend				
T_c	0%	5%	10%	20%	30%
119[a]	4.7		4.05	3.78	3.85
121[a]	3.25		3.15	2.73	2.68
123[a]	2.25		2.21	1.90	1.76
125[a]	1.52		1.39	1.30	1.27
127[a]	1.03		0.89	0.94	0.85
129[a]	0.68		0.66	0.57	0.56
131[a]	0.46		0.42	0.41	0.38
133[a]	0.25		–	0.27	–
135[a]	0.18		0.18	0.17	0.18
119[b]	4.7	4.15	4.02	3.63	3.67
121[b]	3.25	3.15	2.97	2.75	2.82
123[b]	2.25	2.14	2.16	1.98	1.85
125[b]	1.52	1.35	1.36	1.21	1.18
127[b]	1.03	0.98	0.97	0.91	0.84
129[b]	0.68	0.51	0.52	0.67	0.62
131[b]	0.48	0.38	0.38	0.35	0.37
133[b]	0.25	0.25	0.25	0.25	0.26
135[b]	0.18	0.18	0.17	0.18	0.18
137[b]	0.12	0.12	0.10	0.10	0.13
139[b]	0.06	0.08	0.07	0.07	–
141[b]	0.05	0.05	0.05	0.04	0.05
119[c]	4.7	3.80	3.98	3.70	
121[c]	3.25	2.75	2.91	3.00	
123[c]	2.25	1.94	2.28	2.08	
125[c]	1.52	1.42	1.40	1.40	
127[c]	1.03	0.84	0.96	0.90	
129[c]	0.68	0.43	0.46	0.42	
131[c]	0.46	0.27	0.29	0.33	
133[c]	0.25	0.23	–	0.20	
135[c]	0.18	0.10	0.15	0.13	
119[d]	4.7		3.20	2.50	
121[d]	3.25		2.35	1.96	
123[d]	2.25		1.76	1.50	
125[d]	1.52		1.31	0.96	
127[d]	1.03		0.82	0.62	
129[d]	0.68		0.45	0.30	
131[d]	0.46		0.27	0.16	
133[d]	0.25		0.20	0.12	
135[d]	0.18		0.12	0.10	

[a] iPP/Buna blends
[b] iPP/Dutral blends
[c] iPP/Epcar blends
[d] iPP/PiB blends

function of T_c at the given compositions. From these tables it emerges that the dilution of iPP with EPM elastomers causes only a small depression in G. On the contrary, a notable reduction in growth rates on addition of PiB to iPP is observed. At 121 and 125 C, for example, G falls sharply from 3.25×10^{-3} to 1.96×10^{-3} (cm min^{-1}) and from 1.52×10^{-3} to 0.96×10^{-3} (cm min^{-1}) respectively for the iPP PiB (80 20) blend.

Melting behaviour

Figure 6 (*a*, *b*, *c* and *d*) shows the relation between the observed optical melting temperatures T_m' and the crystallization temperatures T_c for iPP and its blends with EPM and PiB elastomers. For each composition the data points can be represented by straight lines in accordance with the relation[11]

$$T_m' = T_m\left[\frac{\gamma - 1}{\gamma}\right] + T_c\frac{1}{\gamma} \qquad (1)$$

where T_m is the equilibrium melting temperature and γ is a morphological factor that turns out to be almost independent of composition and of chemical structure of elastomers (see *Table 6*).

The application of equation (1) to the experimental points in *Figure 6* (*a*, *b*, *c* and *d*) allowed the calculation of T_m. The values are given in *Table 5*.

Mixtures of iPP and EPM elastomers have values of T_m higher than that of pure iPP ($\Delta T_m = T_m - T_m' < 0$). On the contrary, a melting point depression is observed in the case of iPP/PiB blends ($\Delta T_m > 0$) [see *Table 6*].

It is interesting to point out that ΔT_m is a function of composition and of the nature of used elastomer. For example in the case of iPP/EPM blends the larger effect in increasing T_m is obtained by adding Epcar to iPP (T_m = 215 C for iPP/Epcar (80/20) blend while for pure iPP T_m = 197 C).

The behaviour of binary blends at the melting point, with only one crystallizable component, has been studied by various authors who have investigated many systems.

The results, reported in the literature on this matter, show how the dependence of the observed melting point temperature T_m' from T_c may be more complex than that of homopolymers and that the equilibrium melting point T_m can vary, or not with the composition. Some binary systems do not have any depression phenomenon ($\Delta T_m = 0$); this means that T_m' and T_m do not depend on the composition. In this way, the non crystallizable component, neither interacts at the melting point or during the crystallization with the crystallizable component.

The following types of behaviour at the melting point have been noted and reported in the literature, when the blend shows a melting point depression ($\Delta T_m > 0$):

(i) The observed melting temperature, increases linearly with T_c and analogously to what happens to the homopolymer. The slope of the straight line is independent of the composition and of T_c. Assuming equation (1) is valid, this means that the stability or the morphological factor is constant.

The lines extrapolate to values of the equilibrium melting point that are much lower when the concentration of the crystallizable component is higher (see *Figure 7a*).

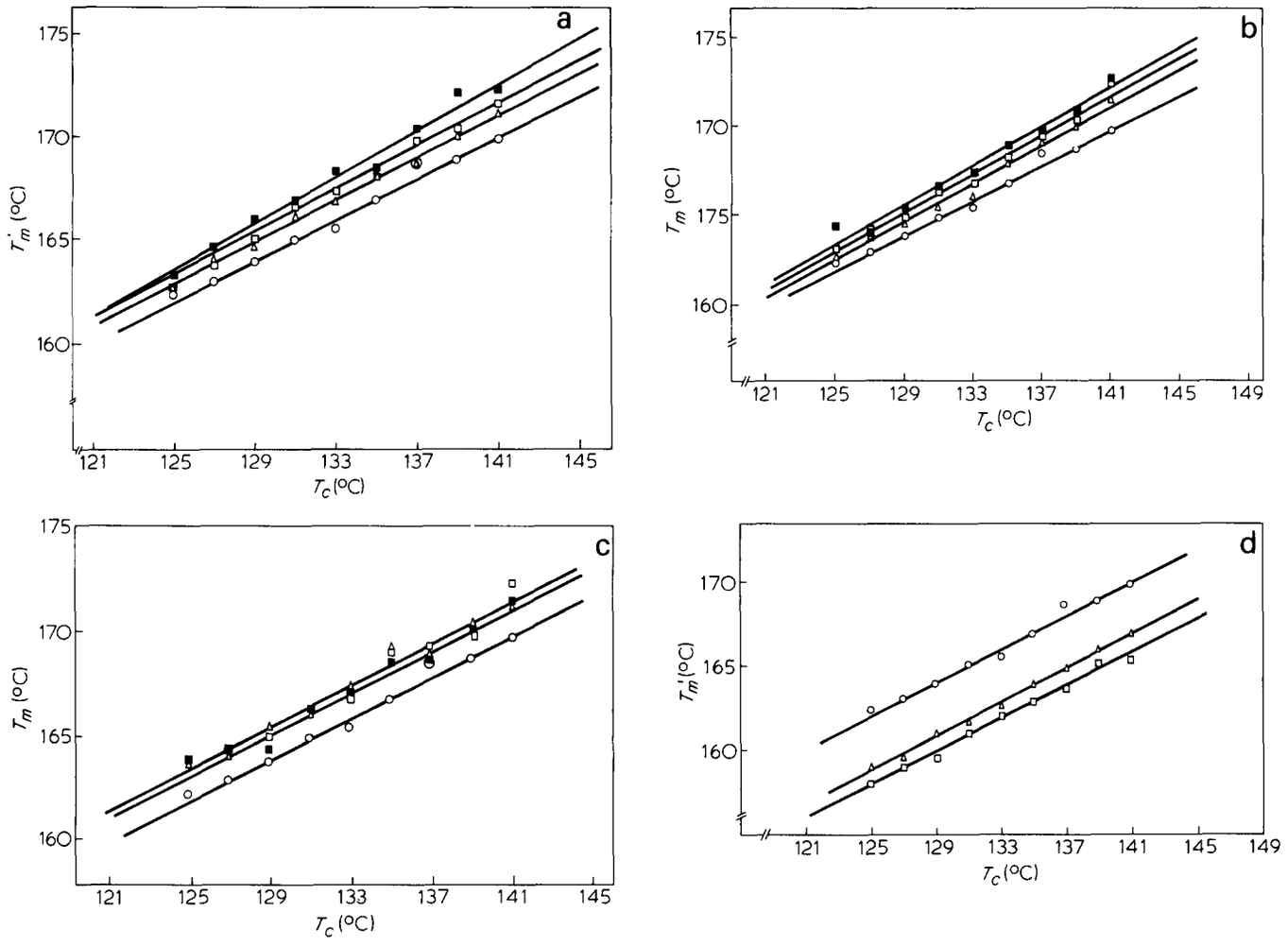

Figure 6 Variation of observed optical melting temperature T_m' with crystallization temperature T_c (a), iPP and iPP/Epcar blends: ⊙, iPP 100%; △, iPP 95%; □, iPP 90%; ■, iPP 80%; (b), iPP and iPP/Dutral blends: ⊙, iPP 100%; △, iPP 90%; □, iPP 80%; ■, iPP 70%; (c), iPP and iPP/Buna blends: ⊙, iPP 100%; △, iPP 90%; □, iPP 80%; ■, iPP 70%; (d), iPP and iPP/PiB blends: ⊙, iPP 100%; △, iPP 90%; □, iPP 80%

(ii) The T_m' of the blends increase linearly with the T_c, and in opposition to the previous case the lines extrapolate to the same T_m value of the homopolymer and their slopes depend on the composition (see *Figure 7b*).

(iii) The T_m' is a linear function of T_c, only for a certain interval of T_c. At high T_c the trend is no longer linear and the depression value is negligible (see *Figure 7c*).

The behaviour of blends belonging to case I, has been interpreted, for low undercooling values, by assuming that the depression of the equilibrium melting point is due to a diluent effect of the non crystallizable component. Therefore the two components must be compatible in the amorphous state for temperatures higher than those of crystallization.

A quantitative analysis of the melting point depression for such systems has been presented by Nishi *et al.*[12] and later by Imken *et al.*[13] based upon a previous treatment elaborated by Scott[14]. The results of this analysis lead to the following equation for ΔT_m:

$$\Delta T_m = -T_m^{\circ}\left[\frac{V_{2u}}{\Delta H_{2u}}\right]BV_1^2 \qquad (2)$$

with

$$B = \frac{RTX_{12}}{V_{1u}} \qquad (3)$$

Table 5 Values of the morphological factor γ for the pure iPP and its blends

iPP	2.0
iPP/Epcar	
95/ 5	2.1
90/10	1.6
80/20	1.8
iPP/Dutral	
90/10	1.9
80/20	1.8
70/30	1.9
iPP/Buna	
90/10	1.7
80/20	1.8
70/30	1.6
iPP/PiB	
90/10	2.0
80/20	2.1

where T_m° is the equilibrium melting temperature of pure crystallizable component; $\Delta H_{2u}/V_{2u}$ is the latent heat of fusion of 100% crystalline polymer per unit volume; V_{1u} is the molar volume of non crystallizable component; X_{12} is

Table 6 Equilibrium melting temperature T_m^0 for iPP and its blends with EPM and PiB elastomer T_m

	T_m (°C); T_m^0	$T_m^0 - T_m' = \Delta T_m$
iPP	197	–
iPP/Epcar		
95/ 5	202	– 5
90/10	207	–10
80/20	215	–18
iPP/Dutral		
90/10	206	– 9
80/20	209	–12
70/30	210	–13
iPP/Buna		
90/10	201	– 4
80/20	204	– 7
70/30	202	– 5
iPP/PiB		
90/10	192	+ 5
80/20	189	+ 8

the Flory–Huggins interaction parameter and V_1 is the volume fraction of non crystallizable component in the melt.

According to equation (2) plots of ΔT_m *versus* V_1^2 should be linear with an intercept at the origin, if there are no entropic contributions to ΔT_m. Entropic contribution gives an additional depression of[15]

$$[\Delta T_m]_s = -R\left[\frac{V_{2u}}{\Delta H_{2u}}\right](T_m^0)^2\left[\frac{\rho_2 \ln V_2}{M_2} + \left(\frac{\rho_2}{M_2} - \frac{\rho_1}{M_1}\right)V_1\right] \quad (4)$$

The entropic term to ΔT_m is normally less than 1 C for components with rather high molecular mass (larger than 10^4)[15]. The equilibrium melting temperature depression observed for blends, compatible in the melt, such as poly(vinylidene fluoride)/poly(methyl methacrylate) (PVF_2/PMMA) and poly(vinylidene fluoride)/poly(ethyl methacrylate) (PVF_2/PEMA) results in a linear function for the composition according to equation (2)[12,13,16]. From these plots, the values of the interaction energy density B and of interaction parameter X_{12} were obtained.

The behaviour according to case II (see *Figure 7b*), has been interpreted by Paul and others[13] and Natov and others[13], showing that the depression in the values of T_m' observed under the same condition for T_c, especially at low T_c, is attributed to morphological effects. The crystalline regions are smaller and less perfect than in the absence of non crystallizable component[13].

The blends poly(ethylene oxide)/poly(methyl methacrylate) (PEO/PMMA) show a behaviour at a melting point similar to that for case III[17], schematically illustrated in *Figure 7c*. According to Martuscelli and others[17] this kind of behaviour is interpreted that, for low T_c (linear part of the plot $T_m' - T_c$) the two components are completely miscible in the melt (the non crystallizing component acts as a diluent), at higher T_c the mutual solubility of the components decreases giving rise to the formation of a two-phase system[17].

The melting point behaviour observed for blends iPP/EPM cannot be described in any cases reported so far.

In fact in the literature there are no examples of binary blends with only one crystallizable component, which present an elevation of the melting point temperature, owing to the addition of a non crystallizable component.

Formally, the Nishi–Wang treatment permits an elevation of the melting point (see equation (2)).

In fact a positive X_{12} would determine an elevation of T_m.

A value for $X_{12} > 0$ requires according to the Huggins lattice theory[18] a positive ΔH_{MIX} so in the case of $X_{12} > 0$, in order to allow the two components to be miscible in the

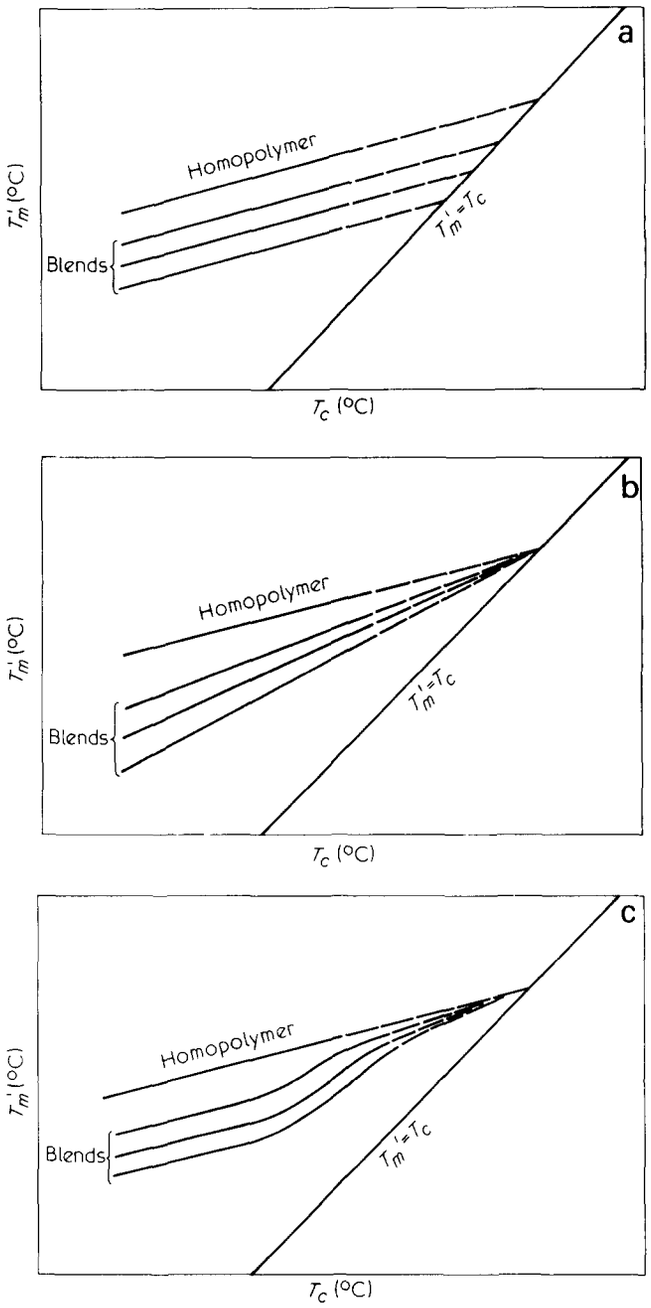

Figure 7 Possible melting behaviours of binary blends with one crystallizable component (schematic): (a) Case I: Blends whose components are compatible in the melt. The melting point depression is caused by a diluent effect. (b) Case II: The observed melting point depression is due to morphological effects. (c) Case III: The blends in this case present reduction phenomena of the mutual solubility in the melt as function of T_c.

Table 7 Mass crystallinity (d.s.c.) of polypropylene phase in iPP/EPM and iPP/PiB blends

Sample	Mass crystallinity (%)		
iPP	31	35	37
iPP/Epcar	35	38	45
(80/20)	+13%	+8.6%	+21.6%
iPP/Dutral	35	36	42
(80/20)	+13%	+2.8%	+11.4%
iPP/Buna	34	36	39
(80/20)	+9.6%	+2.8%	+5.4%
iPP/PiB	30	32	34
(80/20)	–3%	–8.6%	–8.1%
T_c (°C)	125	129	137

melt, i.e. $\Delta F_{MIX} < 0$ and that equation (2) is valid, it will be necessary to verify that the absolute value of term $T\Delta s_{MIX}$ is higher than the enthalpic one. It is well known that, generally, the entropy of mixing of two polymers, is always very low. Then it seems to be improbable to interpret the melting behaviour of iPP/EPM blends on the basis of equation (2) only.

The data reported in *Figure 6a, b, c* can be explained if we assume that during blending the EPM copolymers are able to dissolve a certain amount of iPP molecules having, along the chain, an average higher concentration of chemical defects (steric defects), and molecules with lower molecular mass. In other words, we admit that EPM copolymers may extract selectively from the iPP bulk, more defective molecules, leaving a matrix of iPP molecules having, on average, a higher degree of stereoregularity. The polypropylene matrix would be characterized by a higher melting point and also a higher crystallinity.

In fact, Martuscelli *et al.*[19], studying the melting behaviour of crystals, grown from diluted solutions, of iPP fractions with a different content of isotactic pentads, have shown that the equilibrium melting temperature of iPP, increases as the concentration of sterical defects along the chains diminishes.

The mass crystallinity values of the iPP phase in the iPP/EPM blends, obtained by d.s.c. confirm the above mentioned hypothesis. In fact, as evidenced by *Table 7* data, for the same T_c the iPP matrix crystallinity in iPP/EPM blends is always higher than that of pure iPP.

This effect turns out to be more marked in the case of iPP/Epcar blends. In fact for $T_c = 137$°C an increase in crystallinity of the polypropylene phase, in iPP/Epcar (80/20) blends of 22% is observed; meanwhile iPP/Dutral and iPP/Buna (80/20) show an increase of only 11,4 and 5,4%, respectively. The melting behaviour of iPP/PiB blends agrees with case 1. Consequently, the two components are likely to have a certain degree of compatibility in the melt. Thus PiB acts as a diluent for iPP.

This diluent effect is probably responsible for the depression of the radial growth rate of spherulites observed in the case of iPP/PiB blends.

The temperature dependence of the isothermal growth rate, G, for a pure polymer can be described by the following expression:

$$G = G_0 \exp\left(-\frac{\Delta F^*}{K T_c}\right) \exp\left(-\frac{\Delta\varphi^*}{K T_c}\right) \tag{5}$$

where $\Delta\varphi^*$ is the free energy of formation of a nucleus of critical size, ΔF^* is the activation free energy for the transport process at the liquid–solid interface, K is the Boltzmann constant, T_c is the crystallization temperature and G_0 is supposed to be constant with temperature at least for low values of undercooling. The term ΔF^* is usually taken from the *WLF* time–temperature superposition principle[21] as

$$\Delta F^* = \frac{C_1 T_c}{C_2 + T_c - T_g} = \frac{4120\, T_c}{51.6 + T_c - T_g} \tag{6}$$

where T_g is the glass transition temperature.

The $\Delta\varphi^*$ term, according to the kinetics theory[11], can be expressed as

$$\Delta\varphi^* = \frac{4 b_0 \sigma_u \sigma_e T_m^\circ}{\Delta H_f (T_m^\circ - T_c)} \tag{7}$$

ΔH_f is the enthalpy of fusion, σ_u and σ_e are the lateral and fold surface free energies of the lamellae, b_0 is the distance between two consecutive monolayer fold planes and T_m° is the equilibrium melting point. Then the equation (5) becomes:

$$G = G_0 \exp\left(-\frac{4120}{R(51.6 + T_c - T_g)}\right) \exp\left(-\frac{4 b_0 \sigma_u \sigma_e T_m^\circ}{\Delta H_f \Delta T} \cdot \frac{1}{K T_c}\right) \tag{8}$$

For a polymer–diluent system the equation of spherulite growth rate G must be modified in the following way

$$G = V_2 G_0 \exp\left(-\frac{4120}{R(51.6 + T_c - T_g)}\right) \exp\left(-\frac{4 b_0 \sigma_u \sigma_e T_m^\circ}{K T_c \Delta H_f \Delta T} + \frac{2\sigma_u T_m \ln V_2}{b_0 \Delta H_v \Delta T}\right) \tag{9}$$

where V_2 is the volume fraction in the melt of crystallizable component and ΔH_v is the enthalpy of fusion per unit volume.

The additional terms in equation (9), V_2 and

$$\frac{2\sigma_u T_m \ln V_2}{b_0 \Delta T \Delta H_v}$$

result from the fact that the rate of nucleation is proportional to the concentration of crystallizable units and from entropic contribution to the free energy of a nucleus of critical size respectively. This last additional term is related to the probability of selecting the required number of crystalline polymeric sequences in the blend.

Using the empirical relation $\sigma_u = 0.1\, b_0 \Delta H_v$ the equation of the spherulite growth rate is given in logarithm form as:

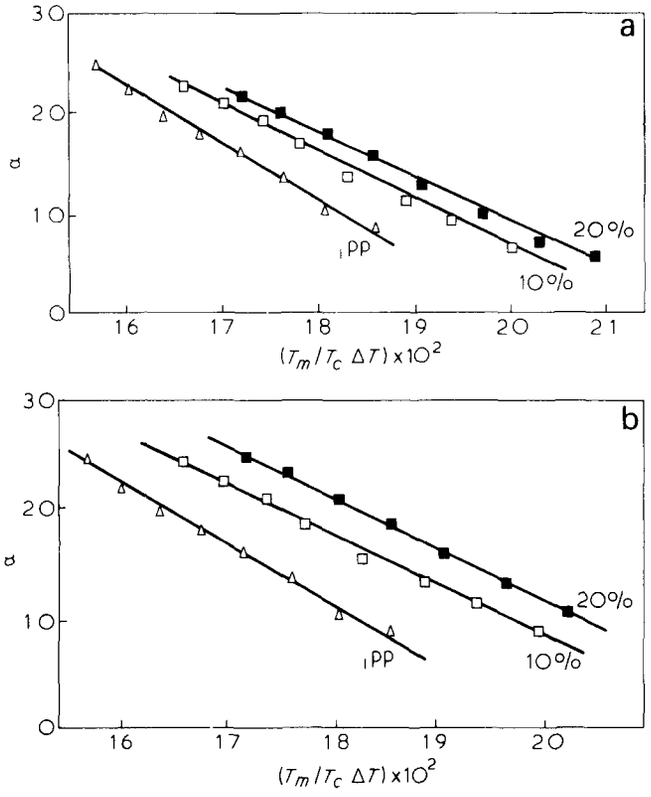

Figure 8 Plots of α against $T_m/T_c\,\Delta T$ for iPP and iPP/PiB blends: (a), $T_g = T_g$ (iPP); (b), $T_g = T_g$ (Fox). The weight percentage of PiB is indicated on the lines

$$\mathrm{Log}G - \mathrm{Log}V_2 + \frac{4120}{2.303R(51.6 + T_c - T_g)} - \frac{0.2T_m(\mathrm{Log}V_2)}{\Delta T}$$

$$= \alpha = \mathrm{Log}G_0 - \frac{0.4\,b_0^2\sigma_e T_m}{2.303\,\Delta T\,K\,T_c} \qquad 10$$

The α term in equation (10) was calculated for iPP/PiB blends in two different ways according that T_g was obtained from the Fox equation[22] or assumed to be constant with composition and equal to that of pure iPP (the following literature data were used: T_g (iPP) = −18°C[23]; T_g (PiB) = −73°C[24]).

To convert weight fractions into volume fractions we used for iPP the density value measured at melting temperature (ρ(iPP) = 0.765 g/cm^3 [25]) and for PiB that measured at 25°C (ρ(PiB) = 0.90 g/cm^3).

As shown in *Figure 8* plots of α against $T_m/T_c\Delta T$ are linear.

From the slopes and the intercepts of these lines σ_e and $\log G_0$ have been calculated. A value of 5.24 Å[27] was used for b_0. As shown in *Table 8*, σ_e and $\log G_0$ seem to be dependent upon composition; in fact both quantities decrease with increasing percentage of non crystallizable component in the blends.

Similar behaviour was observed by Martuscelli *et al.*[17] in the case of PEO/PMMA blends.

The linear trend observed in plots of α against $T_m/T_c\Delta T$ is further convincing evidence of compatibility in the melt between iPP and PiB. The PiB, acting as diluent for iPP, causes an increase in the overall free energy of formation of a nucleus of critical size [see equation (5)]. At the same time a reduction in the value of σ_e is found with increasing the percentage of PiB in the blends. This last result may be accounted for by assuming that the presence of PiB molecules dissolved in the iPP melt may induce an increase in the surface entropy of folding. As a consequence, iPP lamellar crystals with a less regular fold surface are obtained when the iPP/PiB blends are allowed to crystallize isothermally at low undercooling.

Table 8 Values of free energy of folding σe and of $\log G_0$ for iPP and iPP/PiB blends

	σe (erg cm^{-2})		$\log G_0$	
iPP	230*	230**	11.60*	11.60**
iPP/PiB 90/10	193*	192**	10.52*	10.09**
iPP/PiB 80/20	186*	186**	10.56*	10.34**

* $T_g = T_g$ (iPP)
** $T_g = T_g$ (Fox)

REFERENCES

1 Mann, J and Williamson, R. in 'Physics of glassy polymers', (Ed R N Haward), John Wiley and Sons, New York (1973, ch 8), Haward, R N *Br. Polym J* 1970, **2**, 209; Dunn, J R *Rubber Chem Technol* 1976, **49**, 978; Mattiussi, A and Forcucci, F. First Joint Italian–Polish seminar on multicomponent polymeric systems Capri, Italy October 16 21 (1979) (Preprint of short Communications)
2 Horie, K. and Goto, K. *Nippon Gomu Kyokaishi* 1969, **42**, 44
3 Ermilowa, G A, Ragozina, I A and Leont'Eva, N M *Plast. Massy* 1969, **5**, 52
4 Kumbhoni, K J *Polysat Progress (Plast Edn)* 1974, **3**, (Aug-Sept)
5 Spenadel, L *J Appl Polym Sci.* 1972, **16**, 2375
6 Karger-Kocsis, J, Kallò, A, Szafner, A, Bodor, G and Senyei, Zs *Polymer* 1979, **20**, 37
7 Danesi, S. and Porter, R S *Polymer* 1978, **19**, 448
8 Wunderlich, B 'Macromolecular physics', Academic Press, New York, 1973
9 Stein, R S, Khambatta, F. B, Warner, F. B., Russell, T, Escala, A and Balizer, E. *J. Polym Sci. Polym Symp* 1978, **63**, 313
10 Natov, M., Peeva, L and Djagarova, E. *J Polym Sci C*, 1968, **16**, 4197
11 Hoffman, J D *SPE Trans* 1964, **4**, 315
12 Nishi, T and Wang, T. T *Macromolecules* 1975, **8**, 909
13 Paul, D. R. and Altamirano, J. O *Am. Chem. Soc. Adv. Chem. Ser* 1975, **142**, 371; Natov, M., Peeva, L and Djagarova, E *J. Polym Sci Part C* 1973, **16**, 4197
14 Scott, R. L *J Chem. Phys* 1949, **17**, 279
15 Paul, D R. and Barlow, J. W in 'Polymer Alloys II', (Eds. D. Klempner and Kurt C. Frisch), Plenum Press, New York, 1980
16 Kwei, T K, Patterson, G D and Wang, T T *Macromolecules* 1976, **9**, 780
17 Martuscelli, E. and Demma, G in 'Polymeric Blends: Processing-Morphology and Properties', (Eds. E Martuscelli, R Palumbo and M. Kryszewski), Plenum Press, New York (1980)
18 Flory, P J 'Principles of Polymer Chemistry', Cornell University Press, Ithaca, 1953
19 Martuscelli, E, Pracella, M and Zambelli, A *J Polym. Sci., Polym Phys Edn* 1980, **18**, 619
20 Boon, J and Azcue, J M. *J Polym Sci* A-2 1968, **6**, 885
21 Williams, M L., Landel, R F. and Ferry, J D *J Am Chem Soc* 1955, **77**, 3701
22 Fox, T G *Bull Am Chem Soc*, 1956, **2**, 123
23 Manaresi, P and Gianella, V *J Appl Polym Sci.* 1960, **4**, 251
24 Wiley, R H and Braver, G M. *J. Polym Sci* 1948, **3**, 647
25 Danusso, F, Moraglio, G, Ghiglia, W, Motta, L and Todomini, G *Chim Ind* 1959, **41**, 749
26 'Perry's Chemicals Engineers Handbook', Perry, Chilton, Kirkpatrick McGraw-Hill, 1963
27 Martuscelli, E, Pracella, M, Avella, M, Greco, R and Ragosta, G *Makromol Chem* 1980, **181**, 957